AAS 17-626

LOW-THRUST TRANSFER DESIGN BASED ON COLLOCATION TECHNIQUES: APPLICATIONS IN THE RESTRICTED THREE-BODY PROBLEM

Robert Pritchett[*], Kathleen Howell[†], and Daniel Grebow[‡]

Wide-ranging transfer capabilities are necessary to support the development of cislunar space. But, low-thrust transfers between stable periodic orbits are challenging in this regime. Transfer design between such orbits cannot leverage the unstable manifold structures typically employed. Thus, a methodology for constructing these transfers, based on collocation, is demonstrated. Initial guesses comprised of coast arcs along periodic orbits as well as intermediate trajectory arcs from other periodic orbits are converged into feasible transfers and then refined using continuation and optimization strategies. This process applies to various spacecraft configurations and results are validated in a higher-fidelity model. Practical examples demonstrate collocation as a robust approach for computing low-thrust transfers.

INTRODUCTION

An enduring human presence in cislunar space is viewed by NASA and a variety of private organizations as an essential step in the development of a robust space economy and the evolution of manned missions to Mars. Presently, NASA intends to place a space station, the Deep Space Gateway (DSG), in a near-lunar orbit to facilitate the delivery of spacecraft to Mars as well as the lunar surface.[1] Moreover, private industry, e.g., United Launch Alliance (ULA), envisions the development of a self-sustaining economy in cislunar space enabled by a network of transports and propellant depots.[2] These concepts for cislunar facilities require the availability of stable or near-stable orbits in the Earth-Moon (EM) system, orbits that can be maintained for extended intervals with minimal propellant expenditures. Additionally, low-thrust transfers between these orbits are necessary to enable efficient transport of both crewed and cargo spacecraft; for example, NASA proposes transfers of the DSG between cis-lunar orbits of varying geometries using low-thrust propulsion. Low-thrust transfers are also required for a variety of recently considered robotic mission concepts such as the NASA Asteroid Robotic Redirect Mission (ARRM)[3] or lunar cubesat missions.[4] Furthermore, the Earth-Moon system offers a testbed for developing low-thrust techniques to be applied to support low-thrust trajectories in robotic missions to more challenging dynamical regimes such as the Jovian or Saturnian systems. Distant retrograde orbits (DRO) and Near-Rectilinear Halo Orbits (NRHO) in the EM system are examples of stable or nearly stable lunar orbits available for both

[*]Ph.D. Student, School of Aeronautics and Astronautics, Purdue University, 701 West Stadium Avenue, West Lafayette, IN 47907-2045, pritcher@purdue.edu.

[†]Hsu Lo Distinguished Professor of Aeronautics and Astronautics, School of Aeronautics and Astronautics, Purdue University, 701 West Stadium Avenue, West Lafayette, IN 47907-2045, howell@purdue.edu.

[‡]Outer Planet Mission Analysis Group, Mission Design and Navigation Section, Jet Propulsion Laboratory, California Institute of Technology, M/S 264-820, daniel.grebow@jpl.nasa.gov.

manned and robotic mission applications. The abundance of applications for low-thrust transfers in the Earth-Moon system motivates this investigation of design techniques for these transfers that leverage collocation algorithms.

Several authors have investigated strategies for designing impulsive and low-thrust transfers to reach stable and nearly stable periodic orbits in the EM system; however, few have explored general strategies for transfers between such orbits. Investigations of impulsive transfers from the Earth to DROs in the EM system include those by Minghu et al.,[5] Capdevila, Guzzetti, and Howell,[6] as well as Welch, Parker, and Buxton.[7] Capdevila et al. extend this work to develop a network of impulsive transfers between stable periodic orbits in the EM system, including DROs and NRHOs.[8] NRHOs are a subset of the halo family of orbits with stability parameters such that they are classified as stable or nearly stable orbits. These orbits possess lower perilune altitudes and shorter periods than most members of the halo orbit family. Due to these characteristics, Whitley et al. examine impulsive transfers from Earth to NRHOs for human exploration missions.[9] Low-thrust transfers from Earth to DROs are computed by Parker et al.[10] as well as Herman[11] who also develops transfers between DROs. Parrish et al.[12] compute transfers from L_2 halo orbits to DROs, however, the halo orbits employed are beyond the range currently classified as NRHOs. Stable periodic orbits near the Moon offer increasing utility as the development of cislunar space continues, however, transfer design between stable or nearly stable orbits poses unique challenges because the natural dynamical motion often leveraged to guide transfer design formulation is less prominent near stable orbits. Therefore, additional techniques to construct transfers that possess reasonable propellant costs and times of flight are a priority.

This investigation focuses on developing a scheme for computing optimal low-thrust transfers between several types of periodic orbits in the EM system. The direct transcription algorithm as well as the method for initial guess formulation are the foundation for transfer construction in this investigation. Strategies for employing continuation or optimization given a feasible result in the circular restricted three-body problem (CR3BP) are detailed, as well as a scheme for transitioning results to an ephemeris model. Results emerging for a variety of transfer scenarios include a demonstration of leveraging some type of natural dynamical structure in a direct transcription scheme to design transfers. In total, the applications demonstrate that the methodology is practical for generating low-thrust transfers between periodic orbits in the EM system when little information is available for developing an initial guess *a priori*. Transfers between stable periodic orbits are emphasized because these orbits offer the least information for transfer design.

BACKGROUND AND FORMULATION

Circular Restricted Three-Body Problem and Low-Thrust Engine Model

The circular restricted three-body problem (CR3BP) is employed for the initial investigation of low-thrust solutions. The gravitational interaction of the primary bodies in the CR3BP yields low-energy trajectories, i.e., paths that require little propellant because they leverage gravity to the fullest extent; such trajectories are advantageous for low-thrust mission design. Moreover, the CR3BP avoids the complexities inherent in a full ephemeris model, such as time dependence and additional gravitational perturbations, that add complexity to the design process. The CR3BP is defined by three spherically symmetric bodies, two massive primaries, m_1 and m_2, whose mass ratio is represented by, $\mu = m_2/(m_1 + m_2)$, and a third particle whose mass is considered negligible. The primaries are assumed to be in circular orbits about their barycenter and the CR3BP is formulated in a rotating frame. The line from the larger to the smaller body is employed to define the x axis of the

rotating frame. The z axis of the rotating frame is parallel to the orbital angular momentum of the primaries, while the remaining axis is defined by the cross product of the x and z axes. The position and velocity of the third body relative to the system barycenter is typically expressed in a state vector of six Cartesian coordinates, $\boldsymbol{p} = [x, y, z, \dot{x}, \dot{y}, \dot{z}]$, where bold denotes a vector. These six states are employed in the equations of motion for the third body expressed in terms of the rotating frame,

$$\ddot{x} - 2n\dot{y} - n^2 x = -\frac{(1-\mu)(x+mu)}{d^3} - \frac{\mu(x-1+\mu)}{r^3} \tag{1}$$

$$\ddot{y} + 2n\dot{x} - n^2 y = -\frac{(1-\mu)y}{d^3} - \frac{\mu y}{r^3} \tag{2}$$

$$\ddot{z} = -\frac{(1-\mu)z}{d^3} - \frac{\mu z}{r^3} \tag{3}$$

where d and r are scalar distances to the third body, in rotating coordinates, from m_1 and m_2, respectively, and n is the angular velocity of the primary system. To aid numerical computation, states in the CR3BP are typically nondimensionalized using characteristic quantities relevant in the CR3BP system. Thus, the characteristic length, l^*, is equal to the distance between the primaries, while the characteristic time, t^*, is evaluated such that the nondimensional angular velocity of the rotating frame is equal to one. One integral of the motion for the CR3BP exists and is denoted the Jacobi constant, J. This quantity offers useful information about the energy associated with the motion of the third body at a given point, and is defined, $J = 2U - v^2$, where U is the potential of the third body and $v = \sqrt{\dot{x}^2 + \dot{y}^2 + \dot{z}^2}$. In this investigation, the Earth and Moon are employed as the primaries in the CR3BP while the third body represents a spacecraft.

A model for the characteristics of the low-thrust spacecraft must also be defined. In this study, the model for the low-thrust spacecraft assumes an initial mass of $m_0 = 500\ kg$, a maximum thrust of $T_{max} = 100\ mN$, and a specific impulse of $I_{sp} = 2000\ sec$. These parameters are comparable to the Deep-Space 1 and Dawn spacecraft and are achievable with current low-thrust engine technology. The initial mass of the spacecraft defines the characteristic mass, m^*, that is used to nondimensionalize all mass quantities. Following the definition of a suitable dynamical model numerical methods for the computation of low-thrust trajectories within this model must be selected. A variety of numerical techniques are required to compute, optimize, and continue the low-thrust trajectories.

Collocation Framework and Mesh Refinement

Ultimately, low-thrust mission design is a type of continuous optimal control problem, that is, at each instant along a trajectory, a thrust magnitude and direction must be determined that optimize some final parameter, typically propellant mass or time of flight. Numerical methods for solving optimal control problems are incredibly powerful, however, to leverage these techniques, a continuous optimal control problem must be discretized and numerous strategies for this procedure are available. Collocation schemes offer one technique for discretizing the continuous optimal control problem and, when applied for this purpose, the process is denoted direct transcription.[13] A direct transcription approach is employed in this analysis due to its robustness, i.e., such a technique produces solutions even given a poor initial guesses.

Collocation is the core algorithm underlying this strategy for constructing low-thrust transfers between periodic orbits, with a particular focus on transfers between stable orbits. Collocation is a methodology for numerically integrating differential equations and is frequently employed to

transcribe continuous optimal control problems into nonlinear programming (NLP) problems to be solved with direct optimization techniques.[14,15] Direct optimization algorithms leveraging collocation are a proven technique for generating low-thrust solutions when little intuition exists to construct the initial guess. This is because the wide basin of convergence offered by collocation strategies enables successful delivery of solutions even with a poor guess. One sample application is the lunar pole-sitting orbits produced by Ozimek, Grebow, and Howell[16] where the authors introduce a "stack" of nodes in the desired region of the phase space as an initial guess to compute low-thrust pole-sitting orbits. This strategy is aided by the fact that path constraints are straightforward to incorporate into collocation schemes, thus, allowing the final pole-sitting orbits to be bounded in phase space. Similarly, Herman[11] as well as Parrish et al.,[12] demonstrate that a stack of one or more ballistic coast arcs along the departure and arrival orbits supplies a sufficient initial guess for convergence of a collocation algorithm to a numerically continuous transfer solution. Overall, the robustness and adaptability of direct transcription offers a powerful strategy for computing low-thrust solutions between stable periodic orbits.

Collocation algorithms are structured to accurately represent the integration of a set of differential equations by computing polynomials that approximate the numerical propagation of the equations of motion. To ensure the polynomials supply a reasonable approximation, states at specific times along the path constructed via the polynomials are *collocated* with states computed from the differential equations at the same times, i.e., the states produced from each approach must be equal within a desired tolerance. A variety of approaches for implementing a collocation strategy are available; these are distinguished by the degree and node spacing of the polynomials. The node placement strategy impacts the accuracy of the result, thus, in this analysis, a scheme that balances precision with ease of implementation is selected. A Legendre-Gauss (LG) node spacing strategy is employed where the collocation points are determined from the roots of a Legendre polynomial.[17] Additionally, a variable degree polynomial scheme is modeled after those leveraged by Williams[18] as well as Grebow and Pavlak[17] and described by Pritchett,[19] however, 7^{th} degree polynomials are employed unless otherwise noted. The accuracy of a collocation result is improved via the process of mesh refinement that adds and removes nodes along a path. More nodes and, therefore, more polynomials are placed in regions where a solution is highly nonlinear; these additions enable a polynomial representation to offer a more accurate numerical solution. In this investigation, a mesh refinement approach, developed by Grebow and Pavlak[20] and denoted Control with Explicit Propagation (CEP), is utilized. This strategy supplies an accurate result with the added benefit of verifying the solution with a third-party propagator in the process. These collocation and mesh refinement techniques ensure accurate numerical integration of the system differential equations, however, additional problem constraints are still required to enable convergence to a feasible low-thrust solution.

All of the collocation techniques, along with additional constraints, are implemented in a software package that utilizes Collocation with Optimization for Low-Thrust trajectory design and is, thus, denoted COLT. In this software, the collocation framework is implemented via a design variable and constraint formulation that permits the straightforward addition of a variety of problem constraints, e.g. continuity or endpoint constraints. The position vector, $\boldsymbol{x}_{n,p}$, velocity vector, $\dot{\boldsymbol{x}}_{n,p}$, mass, $m_{n,p}$, and four-element control vector $\boldsymbol{u}_n$ comprise the states at the nodes that are employed to construct the collocation polynomials. The complete set of states at all the nodes are the design variables for the low-thrust trajectory design problem. The four control states include the three components of the thrust unit vector, $\boldsymbol{u}_{\hat{T}}$, as well as the magnitude of the thrust vector, $u_{|T|}$. All of these states are

concatenated into a single design variable vector, that is,

$$\boldsymbol{X} = [\boldsymbol{u}_1,\ \boldsymbol{x}_{1,1},\ \dot{\boldsymbol{x}}_{1,1},\ m_{1,1},\ \boldsymbol{x}_{1,2},\ \dot{\boldsymbol{x}}_{1,2},\ m_{1,2}, \ldots, \boldsymbol{u}_n,\ \boldsymbol{x}_{n,p},\ \dot{\boldsymbol{x}}_{n,p},\ m_{n,p}]^T \tag{4}$$

where n is the number of segments into which the trajectory is decomposed, and p is the number of nodes used to construct the polynomial over each segment, e.g. $p = 7$ for a 7^{th} degree polynomial. Note that the four control states are constant along each segment of the trajectory. The design variables are used to evaluate the problem constraints and, when the values of all constraints are driven below a desired tolerance, the collocation problem is solved. The defects, $\boldsymbol{f}_{defect}$, are the primary constraints required in a collocation scheme and ensure that the polynomials match the problem dynamics. Additionally, a Legendre-Gauss node spacing strategy necessitates constraints that enforce continuity between adjacent trajectory segments, $\boldsymbol{f}_{continuity}$, and these are formulated as equalities.

In addition to the continuity and defect constraints associated with a typical collocation framework, the scheme employed in this investigation enforces several other equality and inequality constraints collected in the vectors, $\boldsymbol{F}_{eq}$, and $\boldsymbol{F}_{ineq}$, respectively. The complete set of constraints ensures that all low-thrust transfers are feasible. First, the initial states along the departure orbit as well as the final states on the arrival orbit are fixed, $\boldsymbol{f}_0$ and $\boldsymbol{f}_f$, with the exception of the final mass component. Additionally, the three components of the unit vector reflecting the thrust direction are constrained to yield a unit magnitude, $\boldsymbol{f}_{\hat{T}}$, and the total magnitude of the thrust vector is constrained to be between zero and the specified maximum thrust value, $\boldsymbol{f}_{|T|}$. When necessary, minimum altitude constraints, $\boldsymbol{f}_{alt}$, relative to the primary and secondary bodies, are enforced that prevent the final path from possessing a node that is less than a user-defined distance from the center of each body. Altitude constraints are necessary, not only because they ensure a trajectory does not pass through a given body, but because such constraints also alleviate the numerical difficulties that occur due to less predictable nonlinear behavior when a path passes very near a massive body. All of these constraints are concatenated into the vectors of equality and inequality constraints.

$$\boldsymbol{F}_{eq} = \begin{bmatrix} \boldsymbol{f}_{defect} \\ \boldsymbol{f}_{continuity} \\ \boldsymbol{f}_0 \\ \boldsymbol{f}_f \\ \boldsymbol{f}_{\hat{T}} \end{bmatrix} \qquad \boldsymbol{F}_{ineq} = \begin{bmatrix} \boldsymbol{f}_{|T|} \\ \boldsymbol{f}_{alt} \end{bmatrix} \tag{5}$$

For a process that does not involve an optimizer, the inequality constraints are enforced as equality constraints using slack variables. However, when an optimizer is employed, slack variables are handled within the optimizer, thus, altitude constraints are input as inequality constraints. Furthermore, when a transfer is optimized, upper/lower bounds on the design variables are imposed to constrain the thrust magnitude and to limit each mass variable to remain bounded between the initial spacecraft mass and zero. Together these constraints and bounds ensure that COLT generates a practical low-thrust trajectory.

Once the design variable and the constraint vectors are constructed, these vectors along with their gradient, $D\boldsymbol{F}(\boldsymbol{X}_i)$, are employed to compute an update to the design variables. When no optimizer is employed, the minimum-norm equation supplies the update to the design variables, that is,

$$\boldsymbol{X}_{i+1} = \boldsymbol{X}_i - D\boldsymbol{F}(\boldsymbol{X}_i)^T[D\boldsymbol{F}(\boldsymbol{X}_i) \cdot D\boldsymbol{F}(\boldsymbol{X}_i)^T]^{-1}\boldsymbol{F}(\boldsymbol{X}_i) \tag{6}$$

where i indicates the update iteration number. However, for an optimal result, the update is determined with a formula unique to the selected optimization algorithm. This expression also incorporates the value and the gradient corresponding to the objective function. In this investigation, the objective function is always equal to the negative of the final mass value, m_f, along the path, and the optimizer works to minimizes this value. The direct transcription formulation that is implemented in COLT is capable of computing optimal low-thrust trajectories given an initial vector of design variables. However, the construction of this design variable vector that serves as the initial guess is a non-trivial step, and is a primary focus of this investigation.

Initial Guess Construction

All differential corrections approaches employed in transfer design require an initial guess; furthermore, for a problem with many more variables than constraints, the structure of the initial approximation can significantly influence the nature of the result. Currently, one of the key challenges in designing transfers between stable and nearly stable orbits is the general lack of intuition concerning the structure of an initial guess. Compounding the difficulty in the CR3BP is the fact that stable periodic orbits do not possess the invariant manifold structures that often guide the development of an initial guess in a multi-body regime. The solution space available for a transfer is typically comprised of one or more feasible solutions, each with a unique basin of convergence. When the input to a corrections algorithm lies within the desired basin, the corrections process yields a solution with similar characteristics. However, with the existence of many local solutions, the initial guess for the transfer might be significantly altered, resulting in a trajectory without the preferred characteristics. Given the infinite number of potential initial guesses available and the sensitivity of the final solution to the initial guess, a systematic approach for constructing initial guesses and exploring different basins of convergence is critical.

Since little intuition concerning the design space exists, it is advantageous to employ a simple method for initial guess construction that allows rapid exploration of many possible options. A "trajectory stacking" approach, similar to the fundamental technique in Herman,[11] Parrish et al.,[12] Pavlak,[21] and Vaquero[22] is leveraged to formulate an initial guess. In this application, a number of ballistic revolutions are stacked along the departure and arrival orbits such that the states along these revolutions are concatenated into a single design vector that is passed as input to the collocation algorithm. This approach is straightforward and results in an initial guess that is dynamically feasible apart from the large discontinuity between the departure and arrival orbits. A simple example demonstrates the construction of a transfer between predetermined libration point orbits. The sample departure and arrival orbits are plotted in Figure 1(a) for a transfer from a L_2 halo orbit with a Jacobi constant value, $J = 3.0275$, and perilune radius $r_p = 34,688.62\ km$ to an L_1 halo orbit with, $J = 3.0275$, and perilune radius $r_p = 27,102.02\ km$. To construct an initial guess, two revolutions along each halo orbit are stacked resulting in a total flight time equal to 48.2 days. The initial guess is passed to COLT to converge to a feasible transfer as plotted in Figure 1(b). This transfer is computed quickly from an initial guess that contains almost no information concerning the characteristics of the low-thrust transfer between the two halo orbits, demonstrating the effectiveness of this simple initial guess generation method.

The trajectory stacking approach for generating an initial guess is easily modified to explore different basins of convergence for feasible transfers between periodic orbits. Additional trajectory arcs are straightforward to incorporate between the stacked revolutions, to "guide" the initial guess to a particular solution. In this approach, denoted the "orbit chaining method", states along inter-

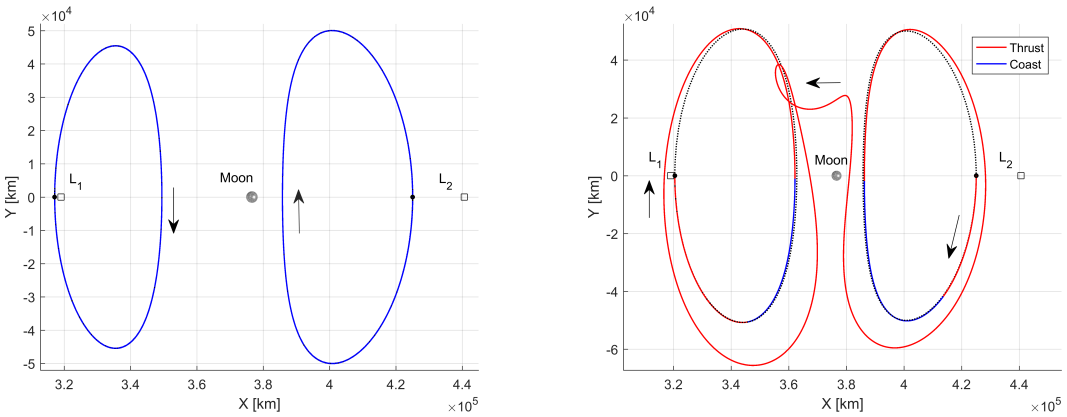

(a) Initial Guess

(b) Feasible Transfer

Figure 1: Feasible L_2 to L_1 halo orbit low-thrust transfer in an Earth-Moon CR3BP model for a spacecraft with an initial mass of 500 kg and engine characteristics such that $T_{max} = 100\ mN$ and $I_{sp} = 2000\ sec$. Time of flight is 47.5 $days$.

mediate trajectory arcs are added to serve as links between the states along the departure and arrival orbits. Such additional trajectory arcs can incorporate a natural dynamical structure, e.g., a periodic or resonant orbit. The choice of intermediate trajectory arcs influences the characteristics of the converged solution, allowing arcs to guide the solution to different basins of convergence. Moreover, optimal low-thrust transfers frequently appear to leverage natural dynamical motion, thus, it is possible that ballistic intermediate trajectory arcs can assist an optimizer in converging to a desired type of local optimal solution. Overall, the robustness and adaptability of a collocation scheme, combined with the flexibility of the trajectory stacking and orbit chaining techniques, offers a powerful strategy for computing low-thrust solutions between stable periodic orbits.

Optimization

Typically, low-thrust mission design ultimately seeks, not just a feasible transfer, but an optimal path. Optimizing a spacecraft trajectory for minimum time or maximum final propellant mass can reduce mission cost and increase scientific return. In direct transcription, an optimal low-thrust trajectory is constructed by pairing a collocation scheme with an optimization algorithm. In this scenario, the collocation scheme supplies the framework for the constraints that ensure a trajectory is feasible, while the optimization algorithm enforces the conditions that ensure an optimal final solution. Numerous optimization algorithms are available and each differs primarily in the particular optimization conditions that are enforced and their implementation. In this investigation, the optimization algorithm SNOPT (Sparse Nonlinear OPTimizer) is employed to construct the optimal solutions.[23,24] Such an optimizer implements a sequential quadratic programming (SQP) optimization approach and is well-suited for the type of large-scale NLP problems produced by direct transcription. The parameters introduced for a particular optimizing strategy must be selected appropriately to deliver a well-scaled problem, and to avoid lengthy convergence times and/or a lack of convergence.

Several techniques are employed to aid in the convergence of the SNOPT algorithm and the delivery of a local optimal solution. First, each element in the vector of design variables, $\boldsymbol{X}$, that

is passed to SNOPT, is assigned upper, $\boldsymbol{X}_{up}$, and lower, $\boldsymbol{X}_{low}$, bounds to restrict the scope of the optimization problem. As discussed previously, the design variable bounds for thrust magnitude and mass remain consistent with those in the problem formulation. Additionally, since no single component of the thrust direction unit vector can possess a value greater than one, these states are bounded to be between zero and one. The bounds for the remaining position and velocity variables are a function of their values in the initial guess, that is, a maximum position, $\boldsymbol{\nu}_{pos}$, or velocity, $\boldsymbol{\nu}_{vel}$, variation from the initial guess is specified,

$$\boldsymbol{X}_{up} = \begin{bmatrix} u_{1_{|T|_{up}}} \\ \boldsymbol{u}_{1_{\hat{T}_{up}}} \\ \boldsymbol{x}_{1,1_{up}} \\ \dot{\boldsymbol{x}}_{1,1_{up}} \\ m_{1,1_{up}} \\ \vdots \end{bmatrix} = \begin{bmatrix} T_{max} \\ \mathbf{1} \\ \boldsymbol{x}_{1,1_0} + \boldsymbol{\nu}_{pos} \\ \dot{\boldsymbol{x}}_{1,1_0} + \boldsymbol{\nu}_{vel} \\ m_0 \\ \vdots \end{bmatrix} \quad \text{and} \quad \boldsymbol{X}_{low} = \begin{bmatrix} u_{1_{|T|_{low}}} \\ \boldsymbol{u}_{1_{\hat{T}_{low}}} \\ \boldsymbol{x}_{1,1_{low}} \\ \dot{\boldsymbol{x}}_{1,1_{low}} \\ m_{1,1_{low}} \\ \vdots \end{bmatrix} = \begin{bmatrix} 1\text{e}{-10} \\ \mathbf{-1} \\ \boldsymbol{x}_{1,1_0} - \boldsymbol{\nu}_{pos} \\ \dot{\boldsymbol{x}}_{1,1_0} - \boldsymbol{\nu}_{vel} \\ 0 \\ \vdots \end{bmatrix} \tag{7}$$

where $\boldsymbol{x}_{1,1_0}$ and $\dot{\boldsymbol{x}}_{1,1_0}$ are the initial values for the position and velocity states at the first node along the first segment. Note that the minimum bound on $u_{|T|}$ is not set exactly to zero to prevent numerical difficulties that may occur when the thrust magnitude equals exactly zero. Reasonable values for $\boldsymbol{\nu}_{pos}$ and $\boldsymbol{\nu}_{vel}$ are selected based on user experience with an optimization problem. Next, the bounds defined for the optimization problem may also aid in further scaling the design variables to ensure all variables are similar in their order of magnitude and, thus, improve the performance of the optimizer, that is,

$$\boldsymbol{s}_{\boldsymbol{X}} = \max\left(|\boldsymbol{X}_{up}|, |\boldsymbol{X}_{low}|\right) \quad \Rightarrow \quad \boldsymbol{X}_s = \boldsymbol{X}/\boldsymbol{s}_{\boldsymbol{X}} \tag{8}$$

where $\boldsymbol{s}_{\boldsymbol{X}}$ is the vector of scaling factors for the design variables and $\boldsymbol{X}_s$ is the vector of scaled design variables after the scaling factor is applied. All the design variables that are input to the optimization algorithm are scaled, however, these variables are not scaled when employed within the constraint or objective functions that are employed by SNOPT. The final technique to aid the convergence of the optimizer is a scaling of the constraints. Although constraint values can exhibit very different orders of magnitude, the constraint tolerance for SNOPT is defined by a single quantity. To ensure that the desired level of accuracy is achieved in an optimized solution, scaling factors for each type of constraint are produced using the following expression,

$$s_F = \frac{err_{tol}}{f_{tol}} \tag{9}$$

where s_F is the constraint scaling factor, err_{tol} is the desired level of error in the constraint, and f_{tol} is the overall feasibility tolerance of the optimization algorithm. For example, if a position constraint must be satisfied to within a 1 meter level of accuracy, then $err_{tol} = 0.001\ km$. Of course, scaling the design variables and the constraints implies that the gradients constructed for the constraints and the objective function must also be scaled. The appropriate scaling factor for each element of the gradient matrix is a ratio of the design variable and the constraint scaling factors relevant to that element. Altogether, bounding the design variables and scaling the constraints as well as the design variables, supports convergence and accurate results in SNOPT.

The feasible transfer from an L_2 halo to an L_1 halo orbit as viewed in Figure 1(b) is input to SNOPT for optimization and the resulting trajectory is plotted in Figure 2(a). The low-thrust transfer

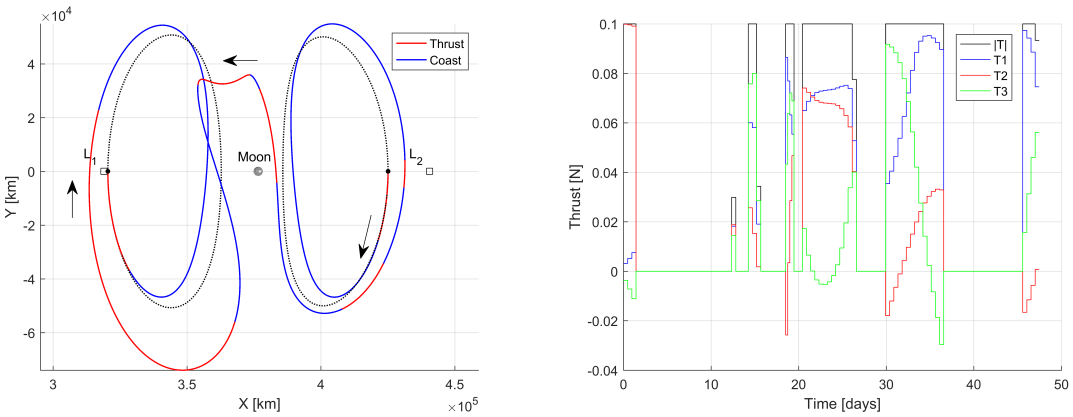

(a) Optimal Transfer

(b) Optimal Thrust Profile

Figure 2: Optimal L_2 to L_1 halo orbit low-thrust transfer in an Earth-Moon CR3BP model for a spacecraft with an initial mass of 500 kg and an engine with $T_{max} = 100\ mN$ and $I_{sp} = 2000\ sec$. Time of flight is 47.5 $days$.

in Figure 1(b) includes a change in mass equal to $\Delta m = 9.85\ kg$ while the optimal transfer in Figure 2(a) emerges with $\Delta m = 8.02\ kg$, therefore, optimizing the trajectory resulted in a mass savings of $1.83\ kg$ as generated in the lower-fidelity CR3BP model. Examination of the thrust profile for an optimal low-thrust solution offers insight on the optimality of the solution. An optimal thrust profile generally exhibits gradual transitions in the thrust pointing direction, as apparent in Figure 2(b), in contrast to the arbitrary and substantial modification in thrust pointing often seen in a feasible solution.

Once a single feasible or optimal low-thrust transfer is produced, it can be employed to generate an entire family of related transfers through a continuation process. One such straightforward technique is natural parameter continuation. This procedure involves incrementally modifying a single parameter in a low-thrust solution and reconverging the solution between each adjustment. The potential continuation parameters for this implementation include maximum thrust, time of flight, and the Jacobi constant value for the departure or arrival orbit. The direct transcription formulation cannot directly optimize any of these parameters, therefore, continuation is employed to construct solutions with more desirable values for these parameters. Together, optimization and continuation techniques are used to explore regions in the solution space and identify the trajectory that best meets a set of desired characteristics.

Transition to Ephemeris Model

The CR3BP offers a convenient model for developing low-thrust transfers, however, these transfers must be validated in an ephemeris model. Selected low-thrust transfers that are originally produced in the CR3BP are reconverged and plotted in an ephemeris model to demonstrate the strategy for future applications. The mission design and navigation software MONTE (Mission Analysis Operation and Navigation Toolkit Environment), developed at the Jet Propulsion Laboratory, is employed to accomplish this task.[25] The MONTE software is a publicly available Python library with a wide array of astrodynamics tools and, among many other capabilities, it facilitates computations in a full ephemeris model. The MONTE sublibrary *MColl* is a framework to compute low-thrust

trajectories within the MONTE environment using direct transcription, and this tool is leveraged to converge low-thrust trajectories in an ephemeris model.[26] The *MColl* algorithm sets up the direct transcription problem with an approach similar to COLT; the primary differences include the fact that *MColl* uses Legendre Gauss Lobatto (LGL) node spacing to construct the polynomials and the open source optimizer IPOPT (Interior Point OPTimizer) to compute optimal trajectories.[27] Due to the basic similarities, it is straightforward to generate trajectories in a CR3BP model with COLT and import them into *MColl* to be converged in a full ephemeris model.

To transition solutions from COLT to *MColl*, a trajectory is first imported and assembled as a trajectory object in MONTE. If the imported transfer reflects a complex geometry or control history, it may also be reconverged in a MONTE-based CR3BP model. Following this step, but prior to a corrections process in an ephemeris model, the trajectory is transitioned from the rotating frame in the CR3BP to a pulsating-rotating frame defined by the ephemerides. In an ephemeris model, to accommodate the fact that the distance between the Earth and the Moon changes continuously, the characteristic quantities are no longer assumed to be constant in the pulsating-rotating frame. To account for this correspondence between the characteristic length and the epoch, the nondimensional states along the trajectory as computed in the CR3BP, are dimensionalized using the constant characteristic quantities from the CR3BP; then, these states are nondimensionalized using the instantaneous values corresponding to the characteristic quantities in the pulsating-rotating frame at the epoch time corresponding to the given state. This procedure is applied to import the optimal L_2 halo to L_1 halo transfer into an ephemeris model that includes the Earth and Moon. Furthermore, if the direct transcription problem requires that the initial or final points along a trajectory be fixed to a periodic orbit, then the desired periodic orbits are converged in a full ephemeris model and states on the ephemeris orbits are accessed to constrain the transfer. For example, the L_2 and L_1 halo orbits in the CR3BP are converged in the same ephemeris model employed for the transfer, and the departure and insertion points along the ephemeris orbits are used to fix the beginning and end of the transfer when it is converged in the full ephemeris model. The epochs associated with the departure point, low-thrust transfer, and insertion point must always be assigned in the necessary sequence. For consistency, the ephemeris model used for the design of the low-thrust transfer is nominally assumed to originate at noon on January, 1^{st} 2000, assumes an EME2000 inertial frame, and includes the Earth and Moon.

This specific combination of initial epoch, frame, and model are employed for the L_2 halo to L_1 halo orbit transfer, and all subsequent transfers, in a full ephemeris model to simplify comparisons. The L_2 halo to L_1 halo orbit transfer is converged in an ephemeris model and is plotted in a rotating frame, as well as the EME2000 frame in Figures 3(a) and 3(b), respectively. Clearly, the ephemeris transfer exhibits a similar geometry but is not identical to the result from the CR3BP and requires approximately 13 kg more propellant. The total propellant usage might be reduced with further optimization. Overall, the result demonstrates that constructing initial guesses for low-thrust transfers in the CR3BP and, eventually, transitioning the solutions to the ephemeris models is effective.

SAMPLE APPLICATIONS

Trajectory Stacking Technique

The methodology to compute optimal low-thrust transfers by stacking orbit revolutions to construct an initial guess is first demonstrated with the computation of low-thrust transfers between two pairs of stable or nearly stable periodic orbits. The first pair of stable periodic orbits is a distant retrograde orbit (DRO) and an L_4 short period orbit (SPO). Conveniently, both of these orbits lie

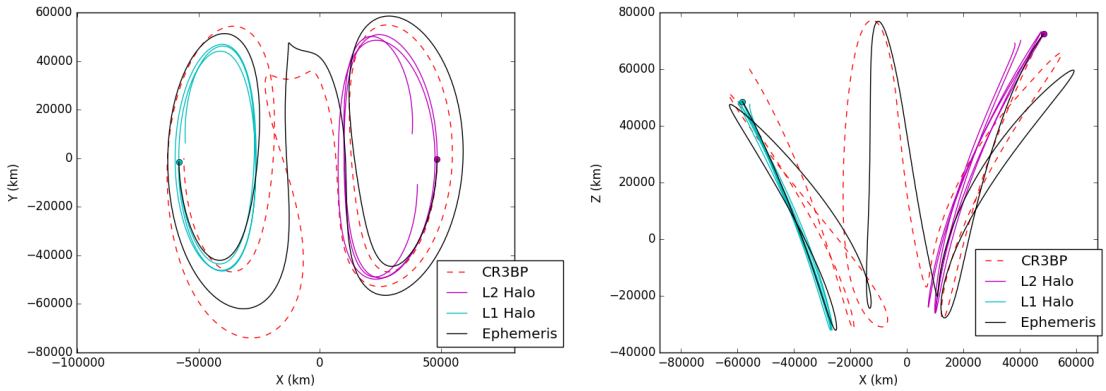

(a) Rotating Frame X-Y Plane

(b) Rotating Frame X-Z Plane

Figure 3: L_2 to L_1 halo orbit low-thrust transfer in a full ephemeris model for a spacecraft with an initial mass of 500 kg and an engine with $T_{max} = 100\ mN$ and $I_{sp} = 2000\ sec$. Time of flight is 47.5 $days$.

entirely in the x-y plane, thus, simplifying the transfer dynamics. The departure DRO and arrival L_4 SPO are selected to possess nearly the same value of the Jacobi constant, i.e., $J = 2.2230$ and $J = 2.2230$, respectively; this similarity further reduces the dynamical challenge of the transfer. The initial guess is constructed with the trajectory stacking approach by concatenating three revolutions of the DRO orbit and two revolutions of the L_4 SPO orbit, resulting in a total time of flight (TOF) equal to 134.8 days. The initial thrust magnitude is zero while the thrust pointing unit vector is assumed to have equal components and unit magnitude. With this initial guess, the collocation algorithm converges to the low-thrust transfer plotted in Figure 4(a) which results in a final spacecraft mass, $m_f = 478\ kg$. The intervals of thrusting and coasting along this transfer successfully guide the spacecraft to the insertion state, however, they appear to be arbitrary in terms of placement. A transfer from the DRO to the SPO that achieves minimum propellant consumption includes thrust and coast arcs located to best leverage the natural dynamics in the EM system. To achieve this result, the feasible solution is passed to the optimization algorithm SNOPT that converges to the solution that achieves the maximum final spacecraft mass for the given transfer time. The optimal transfer produced by SNOPT is displayed in Figure 4(b). This transfer leverages more coast segments as well as thrust segments that employ only the maximum thrust level to achieve a transfer with a delivered mass, $m_f = 482\ kg$. Thus, the optimal transfer consumes approximately $4\ kg$ less propellant than the original feasible result. The locally optimal transfer retains largely the same geometry as the original feasible transfer, however, it is possible that other optimal transfers that may be less costly with drastically different geometries and similar times of flight exist between these two orbits. Computing such transfers requires different initial guesses and perhaps alternative optimization strategies.

The next pair of stable or nearly stable periodic orbits that serve as a sample transfer include a near-rectilinear halo orbit (NHRO) and a distant retrograde orbit (DRO). Transferring between these two orbits requires a significant plane change that increases the complexity. Moreover, the departure NRHO and arrival DRO possess significantly different values of the energy-like Jacobi constant, $J = 3.0347$ and $J = 2.9328$, respectively, and this feature further increases the dynamical

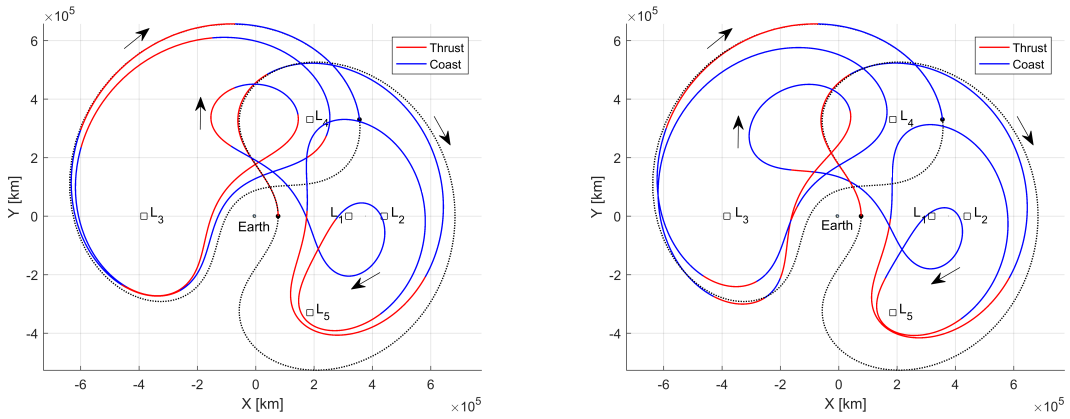

(a) Feasible Transfer

(b) Optimal Transfer

Figure 4: DRO to L_4 SPO low-thrust transfer in the EM system for a spacecraft with an initial mass of 500 kg and an engine with $T_{max} = 100\ mN$ and $I_{sp} = 2000\ sec$. Time of flight is 134.8 $days$.

challenge. The initial guess is constructed with the trajectory stacking approach by concatenating three revolutions of the NRHO orbit and two revolutions of the DRO orbit, and this results in a total time of flight (TOF) of 46.7 days. Given such an initial guess, the collocation algorithm converged to the low-thrust transfer plotted in Figure 5(a) which results in a final spacecraft mass, $m_f = 483\ kg$. Once again, the intervals of thrusting and coasting appear random with brief coasting segments between long thrust segments. The locally optimal low-thrust trajectory computed with SNOPT includes longer coast arcs, and therefore delivers a final mass of $m_f = 486\ kg$, which is approximately 3 kg greater than the initial feasible trajectory. Consistent with the previous example, the bounds placed on the optimization problem yield a locally optimal transfer that retains a similar geometry to the original feasible transfer, however, this result may not occur if an alternate initial guess or dynamical model is employed.

The optimal low-thrust trajectories computed in the CR3BP are transitioned to an ephemeris model to assess their feasibility for mission applications. The low-thrust DRO to L_4 SPO transfer is computed in the same ephemeris model used previously and the resulting feasible trajectory is plotted in the Earth-Moon rotating frame in Figure 6(a). Note that the resulting trajectory possesses a similar geometry to the CR3BP result, however, the inner loops employed to transition to the SPO are shifted in the ephemeris result. Additionally, the ephemeris trajectory requires approximately 18 kg more propellant to achieve, however this is primarily because the ephemeris result is not optimized when converged in the full ephemeris model. The DRO to L_4 SPO transfer converged in the ephemeris model is not optimized because the prototype version of *MColl* is not equipped with the minimum altitude constraints necessary to achieve convergence of an optimal solution. A comparable result is obtained when the NRHO to DRO transfer is converged in the same ephemeris model as is evident in Figure 6(b). In this example, the NRHO to DRO transfer is optimized when converged in the full ephemeris model, and this results in a transfer with a final mass of $m_f = 488\ kg$, that is 2 kg greater than the CR3BP result.

The sample trajectories, demonstrate that a straightforward strategy is available to construct low-thrust transfers between stable or nearly stable periodic orbits for mission applications. Additionally, the characteristics of both of the transfers offered in Figures 4 through 6 suggest that leveraging

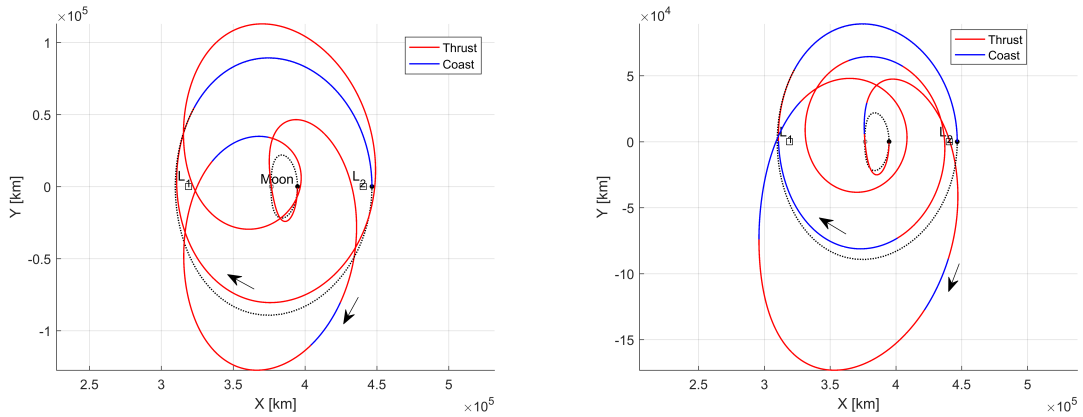

(a) Feasible Transfer (b) Optimal Transfer

Figure 5: L_2 NRHO to DRO low-thrust transfer in the EM system for a spacecraft with an initial mass of 500 kg and an engine with $T_{max} = 100\ mN$ and $I_{sp} = 2000\ sec$. Time of flight is 46.7 $days$.

intermediate trajectory arcs in an initial guess may aid in guiding a transfer to an optimal solution. A notable observation is the fact that various regions along these low-thrust transfer paths resemble other structures in the CR3BP. For example, the large inner loops in Figure 4(b) resemble a resonant orbit or a manifold structure. Initial guess strategies that exploit such similarities may be useful.

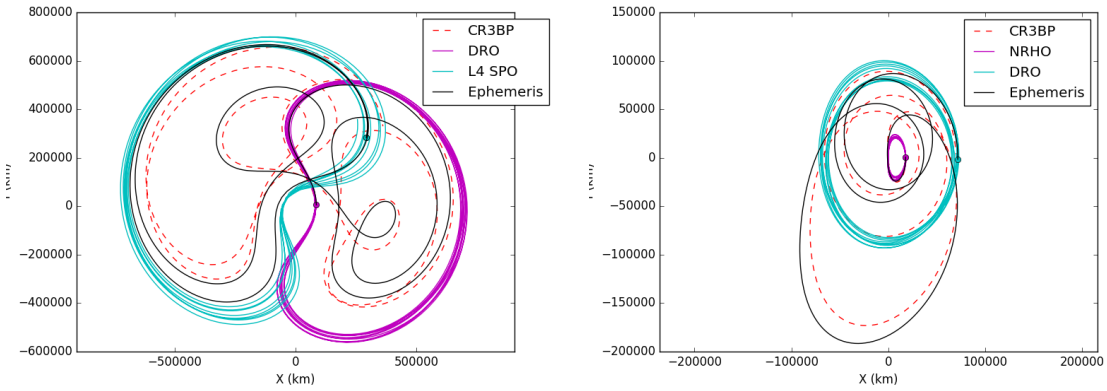

(a) DRO to L_4 SPO Transfer (b) NRHO to DRO

Figure 6: DRO to L_4 SPO low-thrust transfer and a L_2 NRHO to DRO transfer in a full ephemeris model for a spacecraft with an initial mass of 500 kg and an engine with $T_{max} = 100\ mN$ and $I_{sp} = 2000\ sec$. Times of flight are approximately 134.8 $days$ and 46.7 $days$, respectively.

Orbit Chaining Technique

The trajectory stacking technique for initial guess construction is sufficient to yield feasible low-thrust transfers, however, the resulting trajectories are arbitrary and small changes in the problem framework produce vastly different solutions. Thus, to approach transfer design more deliberately,

consider that a significant characteristic that can be ascribed to a transfer is its "itinerary". An approach for the numerical construction of orbits with prescribed itineraries that exploits dynamical chains is developed by Koon et al.,[28] and applied with natural arcs in the three-body problem. The same basic approach is employed here to add trajectory arcs to the initial guess and successfully guide the solution towards desired characteristics. Specific trajectory arcs that leverage the natural dynamics in the CR3BP to reduce the gap between the departure and arrival periodic orbits are selected for inclusion in the initial guess. This approach is similar to leveraging invariant manifolds and natural arcs, to guide transfer design between unstable periodic orbits. Alternatively, low-thrust arcs may bridge the gaps between suitable natural arcs. Without manifolds, families of resonant orbits are one type of orbit that offer structures that span the multi-body system and yield near-connections between a variety of stable periodic orbits. The Adaptive Trajectory Design (ATD) tool is utilized here to generate and explore different families of resonant orbits.[29]

The low-thrust transfers generated with the trajectory stacking technique are reexamined to demonstrate the utility of including an intermediate trajectory arc in the initial guess. The 3:2 family of resonant orbits exhibit geometries that pass near the large DRO, $J = 2.2230$, as well as L_4 SPO, $J = 2.2230$, thus, an orbit from this family is selected for inclusion in the initial guess and appears in Figure 7(a). The intermediate trajectory is selected, not only for its geometry, but because its Jacobi constant value, $J = 2.2115$, is also similar to those of the departure and arrival orbits. A

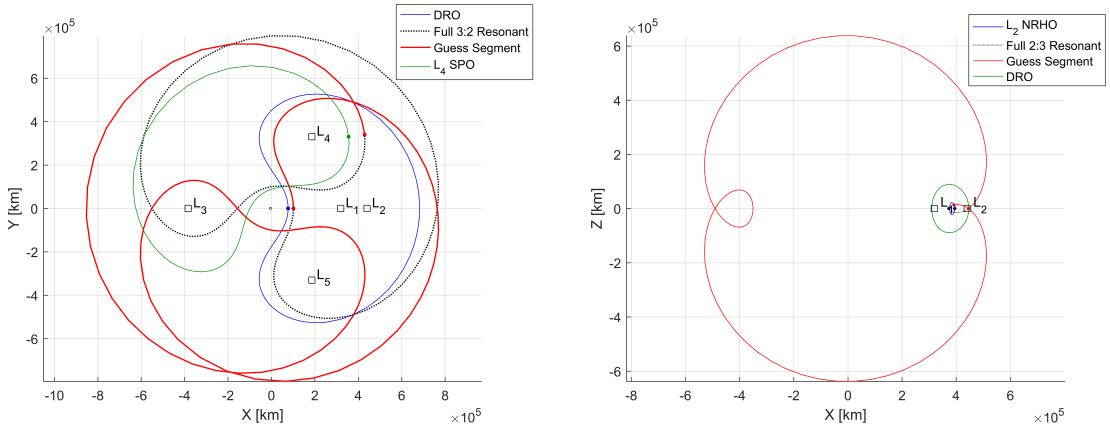

(a) Initial Guess DRO $\rightarrow$ L_4 SPO

(b) Initial Guess NRHO $\rightarrow$ DRO

Figure 7: (a) Initial guess for a low-thrust transfer from a lunar DRO to a L_4 short period orbit that includes a segment of an orbit from the two-dimensional 3:2 resonant orbit family. (b) Initial guess for a low-thrust transfer from a near-rectilinear halo orbit to a lunar DRO that includes a segment of an orbit from the two-dimensional 2:3 resonant orbit family.

ballistic transfer from the DRO to the L_4 SPO must retain this Jacobi constant value. Because the 3:2 resonant orbit is periodic, adding the full orbit in the initial guess yields little benefit, therefore, the trajectory is trimmed to a section that begins and ends where the resonant path passes closest to the departure and insertion locations, on the DRO and L_4 SPO, respectively. The initial guess, then consists of this intermediate arc as well as one revolution about the departure and arrival orbits resulting in a total time of flight of 121.3 days. Optimizing in COLT yields the trajectory in Figure 8. Plotted in the rotating coordinate frame in Figure 8(a), the final transfer is very similar in geometry to the initial guess and this resemblance suggests inclusion of the intermediate arc aided

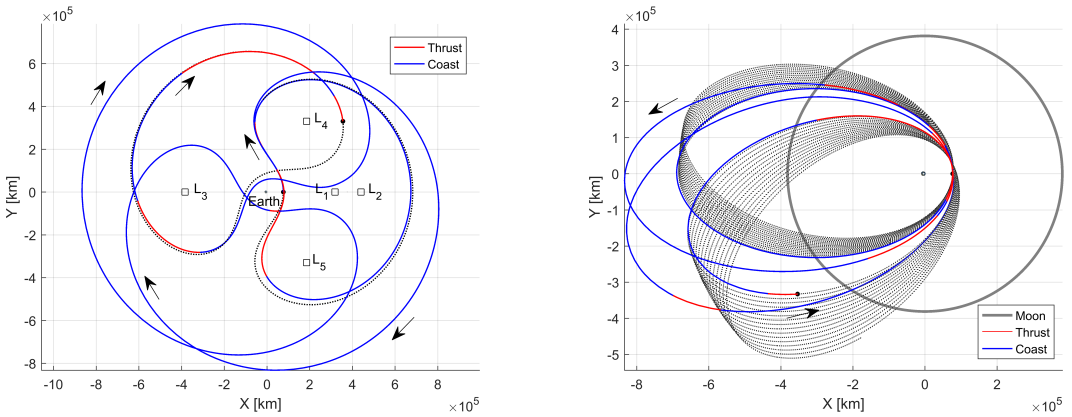

(a) Rotating Frame

(b) Inertial Frame

Figure 8: A low-thrust transfer from a lunar DRO to a L_4 SPO with a total time of flight of 121.3 days plotted in the rotating and inertial coordinate frames. This transfer requires $\Delta m = 3\ kg$.

COLT in computing first, a feasible, and, then, an optimal solution. The thrust arcs along the low-thrust transfer primarily occur during close approaches to the Earth which is most evident when the transfer is plotted in the inertial coordinate frame. The inertial view plot, seen in Figure 8(b), illustrates that the large DRO and L_4 SPO are essentially precessing elliptical orbits relative to the Earth. To complete the transfer, the low-thrust spacecraft utilizes intervals of thrusting at periapse to effect the maximal change in the argument of periapsis. When an intermediate trajectory arc is not employed in the initial guess and an optimal transfer with a similar time of flight is computed, the resulting trajectory is comparable in geometry to the transfer in Figure 4(b). In the former case, the transfer requires a change in mass equal to $\Delta m = 14\ kg$, however, with the intermediate trajectory arc incorporated in the initial guess this transfer requires only $\Delta m = 3\ kg$. This difference indicates that the appropriate leveraging of natural dynamical structures guides an optimizer towards a more optimal low-thrust transfer. However, the difference in performance could also be attributed in part to the number of revolutions in the initial guess, also an indicator of different local optimal solutions.

The transfer from the NRHO, $J = 3.0347$, to the DRO, $J = 2.9328$, from Figure 5 requires a significant plane change, however, a planar 2:3 resonant orbit still appears to be the best candidate from among the families of resonant orbits to add value in developing a near-connection between these two orbits. A 2:3 resonant orbit is selected with a Jacobi constant value, $J = 2.9606$, between those of the NRHO and DRO orbits. The segment along the 2:3 resonant orbit highlighted in Figure 7(b) is incorporated into an initial guess that also includes one revolution along the NRHO and DRO, respectively, resulting in a total time of flight of 96.8 days. The initial guess is passed to COLT which converges to the optimal solution in Figure 9. The view of the transfer in the x-y plane as plotted in Figure 9(a) displays a path that appears similar to the initial guess. However, a view of the transfer that includes the out-of-plane components of the trajectory reveals that the optimization process introduced significant out-of-plane components along the path, as apparent in Figure 9(b). Some shift toward out-of-plane behavior is expected because the departure and arrival orbits are not coplanar, nevertheless, other natural dynamical structures may be better suited for inclusion in the initial guess of this transfer especially ones with some out-of-plane component. The change in mass

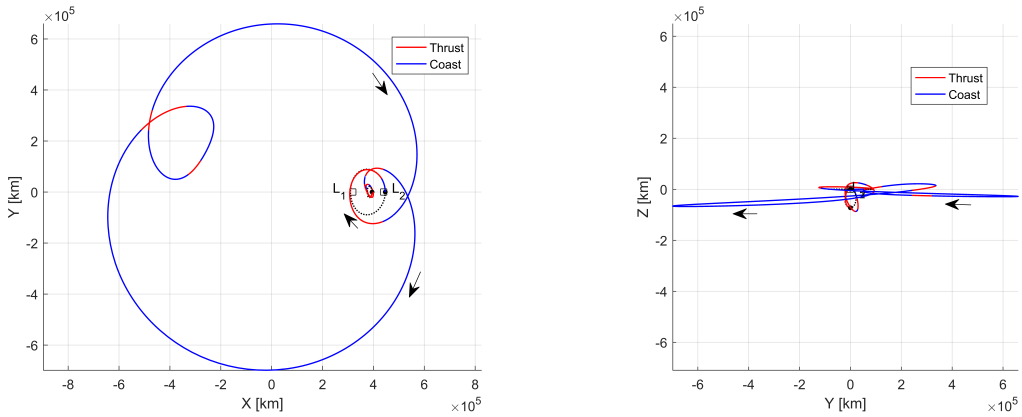

(a) X-Y Plane View (b) Y-Z Plane View

Figure 9: Two views of a low-thrust transfer from a L_2 southern NRHO to a lunar DRO with a total time of flight of 96.8 days. This transfer requires $\Delta m = 12.85\ kg$.

of the optimized transfer in Figure 9(a) is $\Delta m = 12.85\ kg$. This Δm is only $1\ kg$ less than the optimal transfer shown in Figure 4(a) which did not include an intermediate trajectory arc in the initial guess. This small difference in propellant consumption is another indicator that including the selected resonant orbit as an intermediate trajectory arc may not always yield a better initial guess. Both of the transfers generated using the orbit chaining technique are converged in an ephemeris model. The resulting trajectories are plotted in Figure 10 and appear to maintain similar geometries to the CR3BP results. The NRHO to DRO transfer in Figure 10(b) exhibits greater distortion from the CR3BP result, however, the ephemeris transfer maintains the loop structure of the path computed using the lower-fidelity model.

Table 1: Summary of low-thrust transfers examined for a spacecraft with $m_0 = 500\ kg$, $T_{max} = 100\ mN$, and $I_{sp} = 2000\ sec$. The values with * are results computed without optimization in the ephemeris model. The reason for this choice is detailed in the Trajectory Stacking Technique section.

Transfer Type	CR3BP Model		Ephemeris Model
	$TOF\ (days)$	$m_f\ (kg)$	$m_f\ (kg)$
L_2 Halo $\rightarrow$ L_1 Halo	47.5	491.98	491.73
DRO $\rightarrow$ L_4 SPO	134.8	482.03	*463.83
DRO $\rightarrow$ 3:2 Resonant $\rightarrow$ L_4 SPO	121.3	497.04	*472.75
NRHO $\rightarrow$ DRO	46.7	486.14	488.33
NRHO $\rightarrow$ 2:3 Resonant $\rightarrow$ DRO	96.8	487.15	495.00

Applying Continuation to Direct Transcription Results

A natural parameter continuation process is employed to compute a family of low-thrust transfers related by a single parameter, such as maximum thrust or time of flight. When a family of transfer options is obtained, a mission designer can select the transfer that possesses the most desirable characteristics. This technique is first employed here to compute a transfer for a spacecraft with characteristics similar to those proposed for NASA's Deep Space Gateway (DSG) concept. The

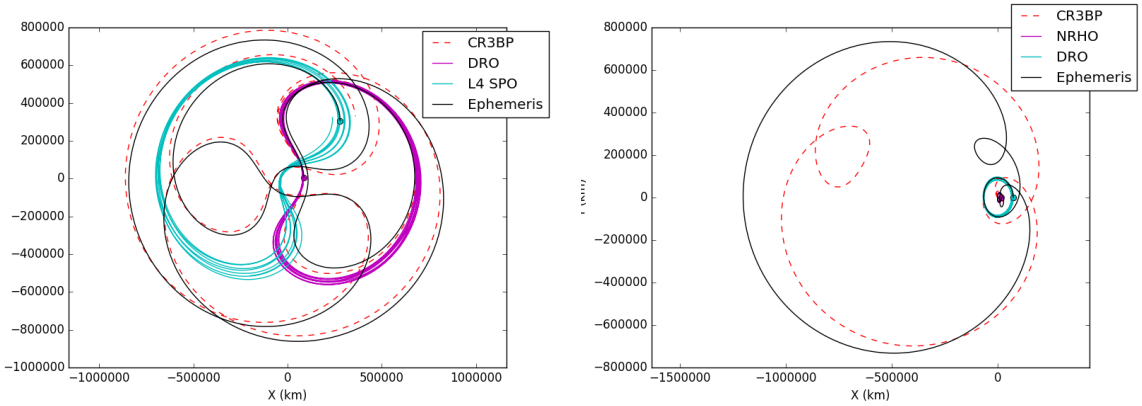

(a) DRO to L_4 SPO with 3:2 Resonant

(b) NRHO to DRO with 2:3 Resonant

Figure 10: DRO to L_4 SPO low-thrust transfer and a L_2 NRHO to DRO transfer in a full ephemeris model for a spacecraft with an initial mass of 500 kg and an engine with $T_{max} = 100\ mN$ and $I_{sp} = 2000\ sec$. Times of flight are approximately 121.3 $days$ and 96.8 $days$, respectively.

DSG is currently planned as a space station equipped with solar electric propulsion, nominally located in a lunar NRHO. Thrust to weight (T/W) ratios for this facility that are currently under consideration range from 1×10^{-6} to 6×10^{-6}. For this investigation, a space station with an initial mass equal to 30 mT and $I_{sp} = 3000\ sec$ is employed, therefore, the permissible range for maximum thrust is $T_{max} = 0.294$-$1.766\ N$. A transfer from a NRHO to a DRO for a spacecraft with these characteristics is the goal, however, the trajectory stacking technique alone is not capable of computing such a transfer because of the small T/W ratio.

Alternatively, a low-thrust transfer with a T_{max} value outside of the desired range is computed and COLT is employed in a continuation scheme to gradually reduce T_{max} to an acceptable value. Initially, an optimal low-thrust NRHO to DRO transfer for a 30 mT spacecraft with $T_{max} = 2.5\ N$ is constructed. A long time of flight is required to achieve this transfer, and this is accomplished either by stacking many revolutions along the initial and final periodic orbits, or by including an intermediate trajectory arc in the initial guess. In this case, a segment from a 2:3 resonant orbit is included in the initial guess because the resulting transfer remains more planar and, therefore, requires less propellant. Next, T_{max} is reduced in 100 mN increments and, at each step, a feasible low-thrust transfer is computed using the result from the previous step as an initial guess; this process continues until reaching a minimum step size. The final feasible low-thrust transfer constructed corresponds to $T_{max} = 1.37\ N$. The transfer constructed with $T_{max} = 1.7\ N$ is selected for optimization and the result is plotted in Figure 11(a). This optimal transfer is also transitioned to an ephemeris model to validate its utility for future mission applications; as plotted in Figure 11(b). This solution demonstrates that low-thrust transfers between lunar orbits with vastly different inclinations are possible for large spacecraft and proves the utility of direct transcription techniques paired with continuation.

The results of a continuation process are also employed to examine a range of possible optimal transfers. In Figures 12(a) and 12(b), a family of optimal low-thrust transfers appears for a range of T_{max} and time of flight values, respectively. Figure 12(a) shows that T_{max} is positively correlated with final spacecraft mass when I_{sp} and time of flight are held constant. Likewise, in Figure 12(b)

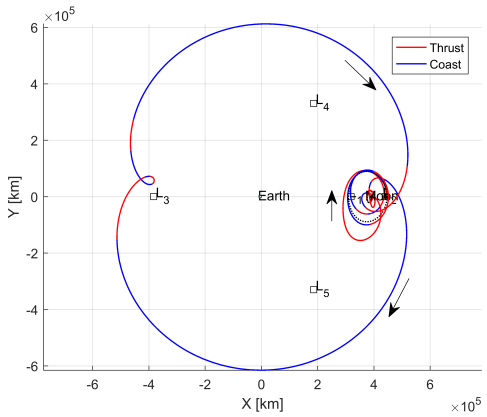

(a) Optimal Transfer in CR3BP

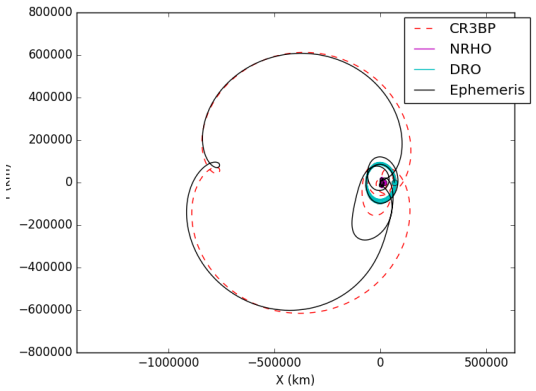

(b) Feasible Transfer in Full Ephemeris Model

Figure 11: Low-thrust transfers for a space station craft with $T_{max} = 1.7\ N$ from a L_2 southern NRHO to a lunar DRO in the CR3BP and full ephemeris models with a total time of flight of 136.2 days. The CR3BP transfer requires $\Delta m = 310\ kg$.

the mass trade-off with time of flight reflects the result that increasing the transfer time of flight leads to less propellant consumption. These results demonstrate that continuation techniques might support exploration of the trade space.

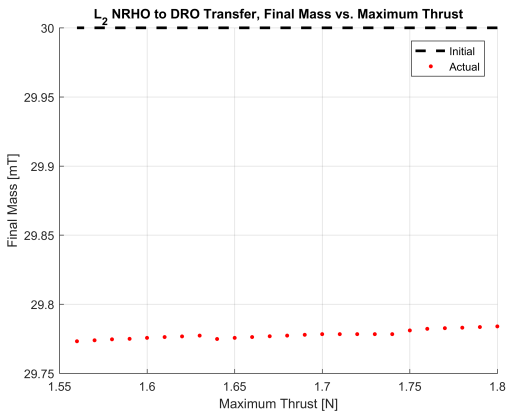

(a) Final Mass vs. T_{max}

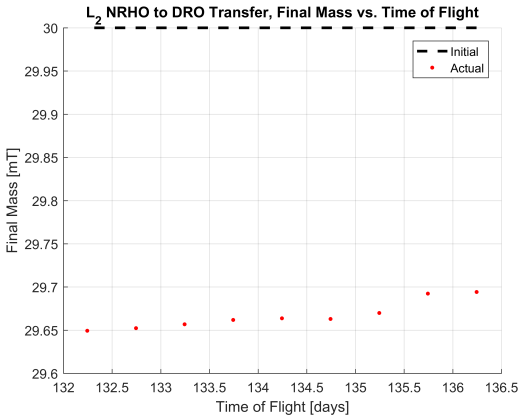

(b) Final Mass vs. TOF

Figure 12: Final mass of optimized low-thrust transfers as a function of two different continuation parameters. All transfers are from a L_2 southern NRHO to a lunar DRO and use a spacecraft with an initial mass of $m_0 = 30,000\ kg$ and $I_{sp} = 3000\ sec$.

CONCLUDING REMARKS

This investigation demonstrates the application of collocation techniques to support low-thrust mission design in the CR3BP. A trajectory stacking technique produces initial guesses with large initial position and velocity discontinuities, however, the robust convergence properties of direct transcription algorithms enable this approach to generate optimal low-thrust trajectories even with a

poor initial guess. The simple trajectory stacking method is particularly well-suited for computing transfers between stable and near-stable periodic orbits because these orbits do not possess invariant manifold structures to guide the formulation of an initial guess. A single low-thrust transfer may also serve as the basis to generate a family of transfers related by a single parameter such as maximum thrust. Any such transfer may be transitioned to a higher-fidelity model where a path with similar characteristics is often available.

Chaining intermediate trajectory arcs between stacked revolutions of the departure and arrival periodic orbits is also a useful strategy for reducing the error in an initial guess and guiding a direct transcription algorithm toward a particular optimal solution. In this investigation, families of resonant orbits supply advantageous trajectory arcs because their geometries intersect the periodic orbits of interest. Likely other transfer scenarios require different types of natural dynamical structures, e.g., periodic orbits, three-dimensional resonant orbits, or invariant manifolds. Fortunately, the orbit chaining strategy is versatile and can incorporate segments from each of these trajectory types. However, while many options for intermediate trajectory arcs are available, not all arcs benefit an initial guess, and sometimes no arc is required. Nevertheless, an orbit chaining approach paired with a continuation scheme can generate low-thrust transfers that would be challenging to design without these strategies. Further development of these methods will facilitate trajectory design in dynamical regimes where little intuition is available for the construction of an initial guess.

ACKNOWLEDGMENT

Gratitude must be extended to Thomas Pavlak, Juan Senent, and Emily Zimovan, for beneficial conversations and suggestions. Portions of this work was conducted at Purdue University and is supported by the NASA Space Technology Research Fellowship, NASA Grant No. NNX16AM42H. Portions of this work was carried out at the Jet Propulsion Laboratory, California Institute of Technology, under a contract with the National Aeronautics and Space Administration. Government sponsorship acknowledged.

REFERENCES

[1] R. Whitley, R. Martinez, G. Condon, J. Williams, and D. Lee, "Cislunar Near Rectilinear Halo Orbits for Human Space Exploration," *Aiaa Space 2016*, 2016.

[2] B. F. Kutter and G. F. Sowers, "Cislunar-1000: Transportation supporting a self-sustaining Space Economy," *AIAA SPACE 2016*, No. 1 in AIAA SPACE Forum, pp. 1–14, Long Beach, California: AIAA, sep 2016.

[3] N. Strange, J. Brophy, F. Alibay, M. McGuire, B. Muirhead, and K. Hack, "High Power Solar Electric Propulsion and the Asteroid Redirect Robotic Mission (ARRM)," *IEEE Aerospace Conference*, Big Sky, Montana, 2017, pp. 1–10.

[4] R. W. Conversano and R. E. Wirz, "Mission Capability Assessment of CubeSats Using a Miniature Ion Thruster," *Journal of Spacecraft and Rockets*, Vol. 50, No. 5, 2013, pp. 1035–1046.

[5] T. Minghu, Z. Ke, L. Meibo, and X. Chao, "Transfer to long term distant retrograde orbits around the Moon," *Acta Astronautica*, Vol. 98, No. 1, 2014, pp. 50–63.

[6] L. Capdevila, D. Guzzetti, and K. C. Howell, "Various Transfer Options from Earth into Distant Retrograde Orbits in the Vicinity of the Moon," *Advances in the Astronautical Sciences*, Vol. 152, No. 1, 2014, pp. 3659–3678.

[7] C. M. Welch, J. S. Parker, and C. Buxton, "Mission Considerations for Transfers to a Distant Retrograde Orbit," *Journal of the Astronautical Sciences*, Vol. 62, No. 2, 2015, pp. 101–124.

[8] L. Capdevila, *A Transfer Network Linking Earth, Moon and the Libration Point Regions in the Earth-Moon System*. Ph.d., Purdue University, West Lafayette, IN, 2016.

[9] R. Whitley, R. Martinez, G. Condon, J. Williams, and D. Lee, "Targeting Cislunar Near Rectilinear Halo Orbits for Human Space Exploration," *AAS/AIAA Astrodynamics Specialist Conference Space 2017*, 2017, pp. 1–20.

[10] J. S. Parker, C. Bezrouk, and K. E. Davis, "Low-Energy Transfers to Distant Retrograde Orbits," *Advances in the Astronautical Sciences Spaceflight Mechanics 2015*, 2015, pp. AAS 15–311.

[11] J. F. C. Herman, *Improved Collocation Methods to Optimize Low-Thrust , Low-Energy Transfers in the Earth-Moon System by*. Ph.d., University of Colorado, Boulder, CO, 2015.

[12] N. L. Parrish, J. S. Parker, S. P. Hughes, and J. Heiligers, "Low-Thrust Transfers From Distant Retrograde Orbits To L2 Halo Orbits in the Earth-Moon System," *International Conference on Astrodynamics Tools and Techniques*, Darmstadt, Germany, 2016, pp. 1–9.

[13] M. Canon, C. Cullum, and E. Polak, *Theory of Optimal Control and Mathematical Programming*. New York: McGraw-Hill, 1970.

[14] J. T. Betts, "Survey of Numerical Methods for Trajectory Optimization," *Journal of Guidance, Control, and Dynamics*, Vol. 21, No. 2, 1997, pp. 193–207.

[15] F. Topputo and C. Zhang, "Survey of Direct Transcription for Low-Thrust Space Trajectory Optimization with Applications," *Abstract and Applied Analysis*, Vol. 2014, 2014, p. 15.

[16] M. T. Ozimek, D. J. Grebow, and K. C. Howell, "A Collocation Approach for Computing Solar Sail Lunar Pole-Sitter Orbits," *Advances in the Astronautical Sciences*, Vol. 135, 2010, pp. 1265–1280.

[17] D. J. Grebow and T. A. Pavlak, "AMMOS Report on Collocation Methods," tech. rep., Jet Propulsion Laboratory, Pasadena, CA, 2015.

[18] P. Williams, "Hermite-Legendre-Gauss-Lobatto Direct Transcription in Trajectory Optimization," *Journal of Guidance, Control, and Dynamics*, Vol. 32, No. 4, 2009, pp. 1392–1395.

[19] R. E. Pritchett, "Numerical Methods for Low-Thrust Trajectory Optimization," Master's thesis, Purdue University, 2016.

[20] D. J. Grebow and T. A. Pavlak, "AMMOS Report on Mesh Refinement for Collocation Methods," tech. rep., Jet Propulsion Laboratory, Pasadena, CA, 2015.

[21] T. A. Pavlak, *Trajectory Design and Orbit Maintenance Strategies in Multi-Body Dynamical Regimes*. PhD thesis, Purdue University, 2013.

[22] M. Vaquero and K. C. Howell, "Leveraging resonant orbit manifolds to design transfers between libration point orbits in multi-body regimes," *Advances in the Astronautical Sciences*, Vol. 148, 2013, pp. 1999–2018.

[23] P. E. Gill, W. Murray, and M. A. Saunders, "SNOPT: An SQP Algorithm for Large-Scale Constrained Optimization," *SIAM Journal on Optimization*, Vol. 12, No. 4, 2002, pp. 979–1006.

[24] P. E. Gill, W. Murray, and M. a. Saunders, "User Guide for SNOPT Version 7," *Office*, Vol. 11, 2008, pp. 1–116.

[25] R. F. Sunseri, H.-C. Wu, S. E. Evans, J. R. Evans, T. R. Drain, and M. M. Guevara, "Mission Analysis, Operations, and Navigation Toolkit Environment (Monte) Version 040," *NASA Tech Briefs*, Vol. 36, No. 9, 2012.

[26] D. J. Grebow and T. A. Pavlak, "MColl: Monte Collocation Trajectory Design Tool," *AAS/AIAA Astrodynamics Specialist Conference*, Stevenson, Washington, 2017, pp. AAS 17–776.

[27] A. Wächter and L. T. Biegler, "On the implementation of an interior-point filter line-search algorithm for large-scale nonlinear programming," *Mathematical Programming*, Vol. 106, Mar 2006, pp. 25–57.

[28] W. S. Koon, M. W. Lo, J. E. Marsden, and S. D. Ross, "Heteroclinic connections between periodic orbits and resonance transitions in celestial mechanics," *Chaos: An Interdisciplinary Journal of Nonlinear Science*, Vol. 10, No. 2, 2000, pp. 427–469.

[29] A. F. Haapala, M. Vaquero, T. A. Pavlak, K. C. Howell, and D. C. Folta, "Trajectory selection strategy for tours in the earth-moon system," *Advances in the Astronautical Sciences*, Vol. 150, Hilton Head, South Carolina, 2014, pp. 1150–1170.